MINERALOGY OF NAKHLITE NORTHWEST AFRICA 14369. P. K. Carpenter[1], A. J. Irving[2], and B. L. Jolliff[1], [1]Dept. of Earth and Planetary Sciences and McDonnell Center for the Space Sciences, Washington University, St. Louis, MO, USA (paulc@wustl.edu); [2]Dept. of Earth & Space Sciences, University of Washington, Seattle, WA, USA.

Introduction: We report the first analytical studies on meteorite Northwest Africa (NWA) 14369, a 247g martian nakhlite from Morocco found in 2021 [1]. It has a cumulate texture and is composed predominantly of euhedral to subhedral prismatic grains of zoned augite (up to 3 mm long) and large (up to 4.5 mm) anhedral grains of zoned olivine together with smaller grains of titanomagnetite (containing pervasive fine ilmenite exsolution lamellae). Augite grains exhibit both simple growth twins and polysynthetic shock twinning; olivine grains contain inclusions of unzoned augite and are crosscut by veinlets of orange-brown "iddingsitic" material. Intercumulus phases are sodic plagioclase (birefringent oligoclase), silica polymorph, alkali feldspar, ilmenite, fluor-chlor-apatite (up to 100 μm in length) and rare baddeleyite and pyrrhotite, plus orange-brown "iddingsitic" material.

Analytical Methods: A bulk polished section of two fragments of the meteorite was studied using backscattered-electron (BSE) imaging, X-ray mapping, and quantitative electron-probe microanalysis (EPMA) using the JEOL JXA-8200 electron microprobe with Probe for EPMA (PFE) operating system at Washington University. Measurements using wavelength-dispersive spectrometry included the mean atomic number background correction, which improves detection and reduces beam damage on sensitive samples. Fluorine was measured with the LDE1 diffracting crystal, with a polynomial background fit to correct for background curvature, and an interference correction for minor overlap of the Fe Lα X-ray line on the F Kα peak. A defocused beam was used for apatite analysis and beam-sensitive behavior of F and Cl X-ray intensities was evaluated using time-dependent intensity emission plots. The halogen analytical protocol and verification of EPMA accuracy was confirmed using Durango and Wilberforce apatite standards. The calculation of halogen site atomic proportions calculations using PFE is in agreement with that of Ketcham [2].

Compositional Maps and Mineral Chemistry: Fig. 1 shows Al-Mg-Fe X-ray intensity maps of the two fragments. These maps illustrate the variability in modal proportions typically observed for nakhlite samples, proportions of cumulate and intercumulus phases, and zoning of the olivine and augite crystals. The mineral chemistry is as follows (averages for cores and rims, ranges for traverses of zoned crystals):

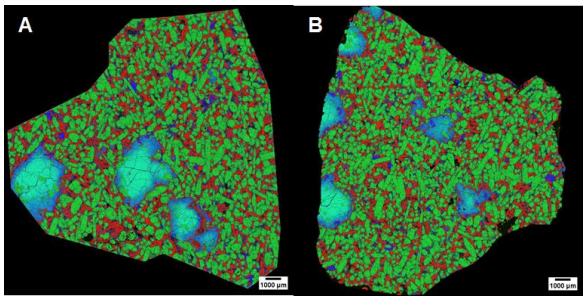

Figure 1. *Nakhlite NWA 14369, thin section samples. A and B Al-Mg-Fe RGB composite X-ray intensity maps. Olivine is light blue with darker blue ferroan rims, augite is green, feldspar is red, and titanomagnetite is dark blue.*

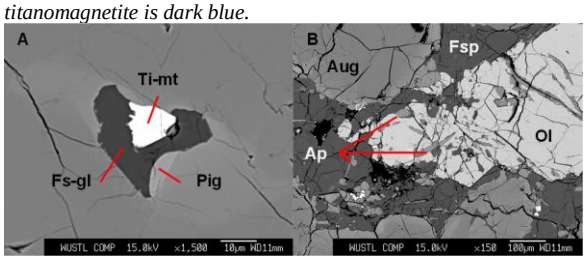

Figure 2. *NWA 14369 BSE images. A: augite magmatic inclusion containing titanomagnetite, pigeonite, and feldspathic glass with submicron apatite. B: olivine, augite, apatite, and feldspar (plagioclase and alkali feldspar).*

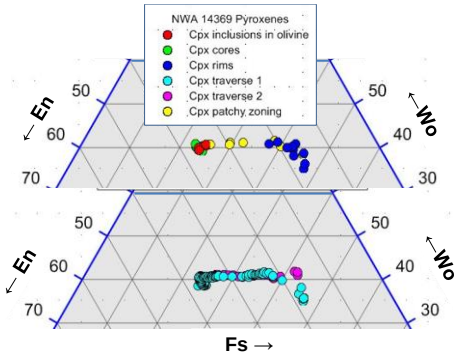

Figure 3. *NWA 14369 Ca-Mg-Fe pyroxene compositions.*

Olivine: cores $Fo_{38.5}$ $Fa_{61.6}$, CaO 0.54 wt.%, FeO/MnO=48, Mg# 0.38, n=6; rims $Fo_{17.7}$ $Fa_{82.3}$, CaO 0.26 wt.%, FeO/MnO=44, Mg# 0.18, n=6; core-rim traverse range $Fo_{38.0\text{-}16.5}$ $Fa_{62.0\text{-}83.5}$, CaO 0.50-0.18 wt.%, FeO/MnO=48, Mg# 0.39-0.17, n=124; intercumulus olivine $Fo_{16.3}$ $Fa_{83.7}$, CaO 0.19 wt.%, FeO/MnO=44, Mg# 0.16, n=5.

Augite: unzoned inclusions in cumulus olivine $Wo_{40.2}$ $En_{35.3}$ $Fs_{24.6}$, FeO/MnO=35, Mg# 0.59, n=5; cumulus zoned augites: cores $Wo_{39.9}$ $En_{36.2}$ $Fs_{23.9}$, FeO/MnO=35, Mg# 0.59, n=10; rims $Wo_{39.1}$ $En_{17.9}$ $Fs_{43.0}$, FeO/MnO=36, Mg# 0.29, n=10; cumulus augite range of patchy zoning $Wo_{40.3\text{-}39.5}$ $En_{36.0\text{-}16.2}$ $Fs_{23.7\text{-}45.4}$,

FeO/MnO=39-41, Mg# 0.26-0.60, n=8. The unzoned augite inclusions in olivine are identical to cumulus augite core compositions. The augite core and rim compositions are documented as discrete analyses and traverses from core to rim of two selected crystals (Fig. 3). The compositional range of augite patchy zoning is similar to the range for core to rim traverses. Augite trace element ranges in oxide wt.% are: TiO_2 0.26-0.79; Al_2O_3 0.73-2.11; Cr_2O_3 0.0-0.41; and MnO 0.43-0.69. Trace element values for unzoned augite inclusions in olivine are similar to cumulate augite core values.

Feldspar: plagioclase: $Ab_{72.8}$ $An_{23.2}$ $Or_{4.0}$, n=5; alkali feldspar: $Ab_{52.6}$ $An_{2.1}$ $Or_{45.3}$, n=5.

Apatite is present as subhedral 100 μm crystals in the intercumulus region, as inclusions in intercumulus olivine, and as sub-micron crystals in augite melt inclusions (Fig 2B). Analysis of 30 intercumulus apatites reveals a range of F-Cl values between two observed limits of (A) F: 3.02 and Cl: 1.29 wt.%, and (B) F: 1.63 and Cl: 3.82 wt.%. These values correspond to atomic formula units of F: 0.82 and Cl: 0.49, and F: 0.45 and Cl: 0.56 per 12 oxygens:

A: $Ca_{4.91}$ $Na_{0.004}$ $Mn_{0.007}$ $Fe_{0.107}$ $Mg_{0.010}$ $P_{2.94}$ $Si_{0.048}$ O_{12} $F_{0.82}$ $Cl_{0.19}$

B: $Ca_{4.94}$ $Na_{0.011}$ $Mn_{0.011}$ $Fe_{0.068}$ $Mg_{0.008}$ $P_{2.94}$ $Si_{0.060}$ O_{12} $F_{0.45}$ $Cl_{0.56}$

These results indicate a negligible amount of OH in the apatite.

Ilmenite: Ilmenite is present as exsolution lamellae in titanomagnetite and as discrete grains, $Fe_{0.98}$ $Ti_{0.98}$ $Mn_{0.03}$ $Mg_{0.03}$ O_3, n=5.

Titanomagnetite: Sub-micron lamellae are present in all titanomagnetite grains. An average of 5 defocused beam analyses and recalculation yields: $Fe^{2+}_{1.38}$ $Fe^{3+}_{1.12}$ $Ti_{0.40}$ $Al_{0.05}$ $Cr_{0.02}$ $Mn_{0.01}$ $Mg_{0.01}$ O_4, with end-member percentages ulvöspinel 41.5 and magnetite 58.5.

Magmatic inclusions: Olivine and augite grains contain magmatic inclusions. The augite melt inclusions contain titanomagnetite, submicron F-Cl apatite, and feldspathic glass (Fig 2A). The inclusion walls have a ferroan augite composition $Wo_{37.0}$ $En_{29.4}$ $Fs_{33.6}$ similar to rim compositions, which zones to pigeonite $Wo_{11.3}$ $En_{26.7}$ $Fs_{62.1}$. The glass contains 0.33-0.53 wt.% Cl with F below detection.

Discussion and Comparison with NWA 13368: The melt which produced NWA 14369 likely crystallized olivine with cotectic crystallization of augite (in part), joined by FeTi-oxide and feldspar. Apatite apparently crystallized with olivine and augite as evidenced by subhedral inclusions in intercumulus olivine. The apatite records a decrease in F with increase in Cl, approximated by apatite A and B. Augite magmatic inclusions contain titanomagnetite, pigeonite, sub-micron F-Cl apatite, and Cl-bearing feldspathic glass. The inclusion wall composition is similar to augite rims, indicating a similar melt chemistry. The pyroxene trend is similar to the trend observed for other nakhlites, yet is distinct in the trend inflection point and degree of enrichment towards ferroan Ca pyroxene compositions (see Fig 3 of [5]).

Nakhlite NWA 13368 is similar to MIL 03346 with augite magmatic inclusions which contain potassic-chloro-hastingsite, Fe sulfide, fayalite, titanomagnetite, and submicron apatite, embedded in Cl-bearing feldspathic glass [3]. The intercumulus region contains skeletal cruciform titanomagnetite and feldspathic glass with submicron apatite. Augite core to rim zoning ranges are: TiO_2: 0.25-1.75, and Al_2O_3: 0.90-4.0, values in oxide wt.%. These textural and compositional features suggest more rapid crystal growth and less diffusion recharge.

In contrast, NWA 14369 is characterized by equant titanomagnetite morphology with pervasive oxidation-exsolution (no skeletal morphologies are observed), and the intercumulus region is dominantly crystalline. Augite zoning of Ti and Al is less pronounced in comparison. These features suggest slower crystal growth and more diffusion recharge, and a comparatively longer cooling history.

The apatite F-Cl range in this study is exhibited within and between crystals, suggesting a relatively continuous evolution of halogen chemistry presumably from apatite A to B. The augite inclusion glass has a similar Cl concentration to intercumulus glass from NWA 13368, and apatite A from this study is similar in composition to intercumulus apatite from that nakhlite. It may be that the elevated K and Fe melt composition of NWA 13368, coupled with available Cl, stabilized amphibole to form in the magmatic inclusions (see [3, 5]), and that these conditions were not attained during crystallization of NWA 14369.

Acknowledgements: We are grateful to Darryl Pitt for obtaining this meteorite specimen and providing material for our research.

References: [1] *Meteorit. Bull. 110* (2021); [2] Ketcham R.A. (2015) *Amer. Mineral., 100,* 1620-1623; [3] Carpenter P.K. et. al. (2020) *52nd LPSC., # 2329;* [4] Treiman A. (2005) *Chemie Erde 65, 203-270;* [5] Jenkins, D.M. (2019) *Amer. Mineral., 104,* 514-524.